Probing the binding of Tb(III) and Eu(III) to the hammerhead ribozyme using luminescence spectroscopy

Andrew L Feig[1]*, Mark Panek[2], William DeW Horrocks, Jr[2] and Olke C Uhlenbeck[1]

Introduction: Divalent metal ions serve as structural as well as catalytic cofactors in the hammerhead ribozyme reaction. The natural cofactor in these reactions is Mg(II), but its spectroscopic silence makes it difficult to study. We previously showed that a single Tb(III) ion inhibits the hammerhead ribozyme by site-specific competition for a Mg(II) ion and therefore can be used as a spectroscopic probe for the Mg(II) it replaces.

Results: Lanthanide luminescence spectroscopy was used to study the coordination environment around Tb(III) and Eu(III) ions bound to the structurally well-characterized site on the hammerhead ribozyme. Sensitized emission and direct excitation experiments show that a single lanthanide ion binds to the ribozyme under these conditions and that three waters of hydration are displaced from the Tb(III) upon binding the RNA. Furthermore, we show that these techniques allow the comparison of binding affinities for a series of ions to this site. The binding affinities for ions at the G5 site correlates linearly with the function Z^2/r of the aqua ion (where Z is the charge and r is the radius of the ion).

Conclusions: This study compares the crystallographic nature of the G5 metal-binding site with solution measurements and gives a clearer picture of the coordination environment of this ion. These results provide one of the best characterized metal-binding sites from a ribozyme, so we use this information to compare the RNA site with that of typical metalloproteins.

Addresses: [1]Department of Chemistry and Biochemistry, University of Colorado, Campus Box 215, Boulder, CO 80309, USA. [2]Department of Chemistry, Pennsylvania State University, 152 Davey Laboratories, University Park, PA 16802, USA.

*Present address: Department of Chemistry, Indiana University, 800 E. Kirkwood Avenue, Bloomington, IN 47405, USA.

Correspondence: Olke C Uhlenbeck
E-mail: olke.uhlenbeck@colorado.edu

Key words: europium, lanthanide, metal binding, RNA, terbium

Received: 21 May 1999
Revisions requested: 6 July 1999
Revisions received: 2 August 1999
Accepted: 11 August 1999

Published: 11 October 1999

Chemistry & Biology November 1999, 6:801–810

1074-5521/99/$ – see front matter

Introduction

The hammerhead ribozyme is a small RNA motif that catalyzes metal-dependent self-cleavage of a unique phosphate bond to give 2′,3′-cyclic phosphate and 5′-hydroxyl termini (Figure 1). As one of the smallest catalytic RNAs, the hammerhead has been the subject of extensive mechanistic [1–5] and structural [6–9] scrutiny. In spite of the wealth of knowledge about this system, the role of the metal ions in maintaining the three-dimensional structure and achieving catalysis remains largely a mystery [10–15]. Metal ion 'rescue' experiments have provided the bulk of our knowledge regarding functional metal ion binding sites [16–18]. In these studies, a hammerhead ribozyme is synthesized containing a sulfur in place of a bridging or nonbridging phosphate oxygen at a unique position. In two cases, this substitution causes loss of activity in the presence of Mg(II), the normal metal cofactor, but adding trace amounts of either Mn(II) or Cd(II) restores catalysis [16–19]. This result suggests that cleavage requires direct coordination of the thiophilic metal ion to the sulfur. Although the rescue experiments imply that a similar interaction occurs between a Mg(II) ion and a phosphate, the experiment is indirect. It is therefore important to have complementary approaches for identifying and studying unique metal-binding sites on RNAs.

We recently showed that the lanthanide ion Tb(III) binds site specifically to the hammerhead ribozyme and inhibits catalysis (Tb = terbium) [20]. Similar experiments have shown that Eu(III) (Eu = europium) is also an effective inhibitor (A.L.F and O.U.C., unpublished observations). The primary Tb(III)-binding site was revealed by using X-ray crystallography. An expanded view of this region (Figure 2) shows that the Tb(III) ion interacts with the Watson–Crick face of guanosine 5. With the exception of the added electron density of the bound Tb(III), no significant changes were observed relative to the native crystal structure. Figure 2 also shows the location of nearby Mn(II) and Mg(II) ions located in separate experiments [6–8]. These ions are sufficiently close to the Tb(III) that they may compete for the site, but they do not share exactly the same coordination environment. G5 is critical for activity of the ribozyme as shown by mutagenesis studies [21–24] and is also involved in a metal-dependent folding transition [25–27]. Verification that this Tb(III) ion is responsible for the inhibition of hammerhead cleavage came from the finding that the incorporation of a bulky 2′-acetamide group at the nearby position 15.3 eliminates Tb(III) inhibition [20]. This effect could result from either completely blocking Tb(III) binding because of the steric bulk of the acetamide moiety or by shifting the position of

Figure 1

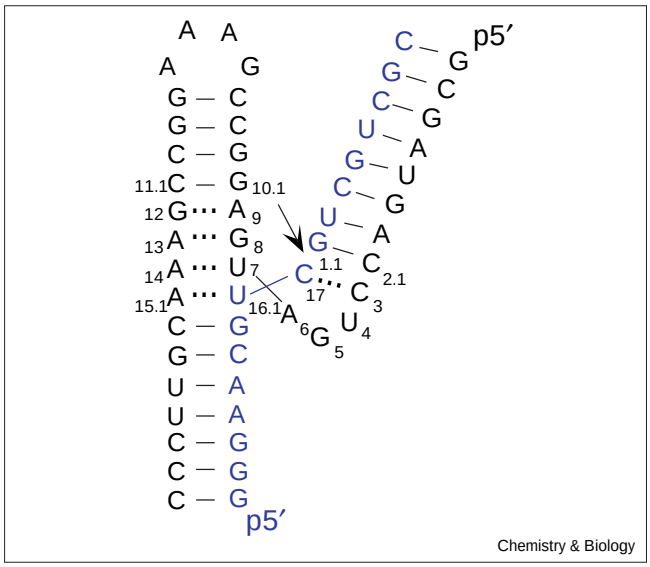

Schematic diagram of the hammerhead ribozymes used in this study.

the Tb(III) ion, making it a less effective inhibitor. This acetamide-modified hammerhead does not show an altered cleavage rate in the absence of Tb(III), suggesting that the Mg(II) ion normally bound to this site does not participate in the approach to the transition state of the reaction. Nevertheless, Tb(III) binding provides an ideal opportunity to study a metal ion that can be biochemically assayed using spectroscopic approaches and helps us to understand the nature of site-specific metal binding by RNAs. In this report we present our studies on the use of luminescence spectroscopy to probe this metal-binding site.

Results

Steady-state luminescence

Sensitized emission spectroscopy allows lanthanide ion binding to nucleic acids to be probed using a standard fluorescence spectrometer [28,29]. The experiment uses the RNA as an antenna for ultraviolet light. If either a Tb(III) or Eu(III) ion is bound to the RNA, resonance energy transfer between the RNA energy donor and the lanthanide ion acceptor occurs. Emission from the long-lived lanthanide excited state is observed: $^5D_4$ in the case of Tb(III) and $^5D_0$ for Eu(III). Figure 3 shows the excitation and emission spectra for Tb(III) bound to the folded hammerhead 16 ribozyme (HH16) [20]. No emission is observed in the absence of either RNA or Tb(III). The fine structure observed in the emission spectrum is typical of Tb(III) luminescence. The other two electronic transitions lead to very weak signals observable under different experimental conditions. A similar emission spectrum is obtained when more concentrated (100–500 μM) Tb(III) solutions are irradiated at 220 nm, conditions under which direct excitation of the Tb(III) ion is observed. Eu(III)

Figure 2

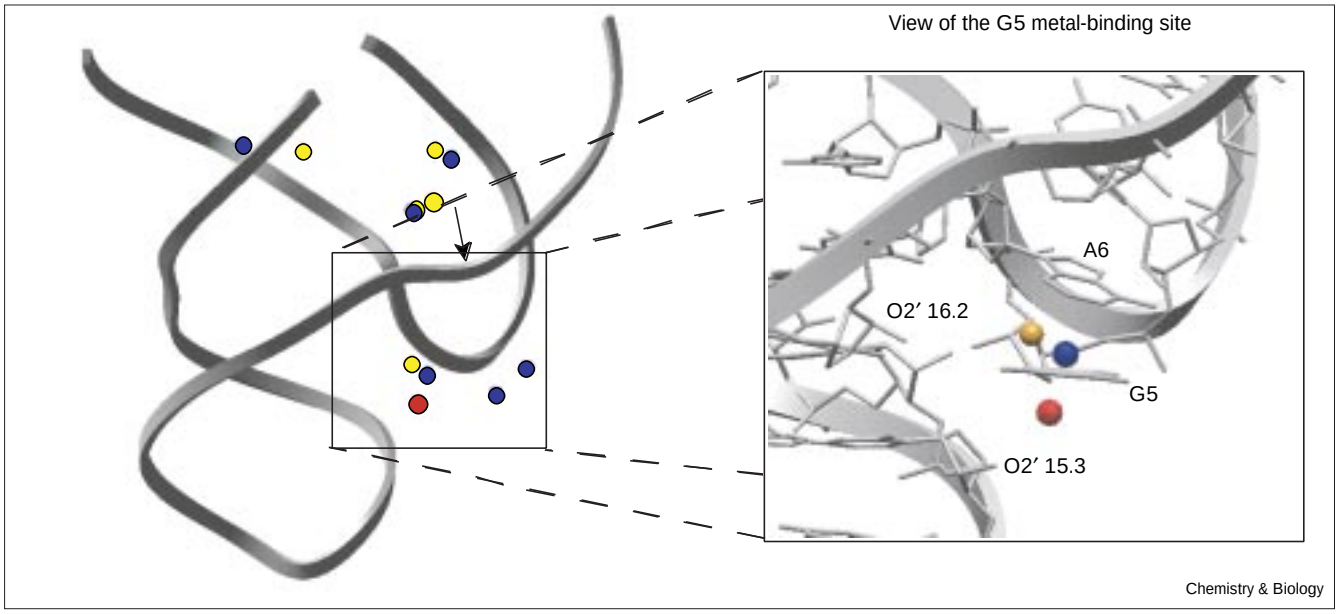

Close-up view of the uridine-turn motif and the metal-binding site adjacent to the base-pairing face of G5. The figure shows the superposition of the three metal ion species that have been observed in this region: Tb(III) is red, Mg(II) is yellow and Mn(II) is blue. Two Mn(II) ions that bind away from the G5 site have been omitted in the expanded view of the region for clarity. Mg(II) and Mn(II) coordinates were obtained from the PDB files URX059 and URX058, respectively. The three metal ions in the G5 site are within ~2 Å of one another, indicating that the binding of any pair of ions would be mutually exclusive.

Figure 3

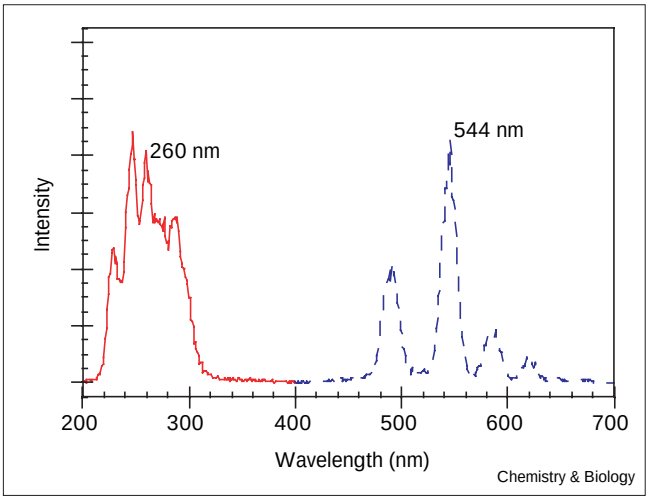

Sensitized luminescence excitation (solid line) and emission (dashed line) spectra for 10 μM Tb(III) binding to 1 μM HH16 (containing a dC residue at the cleavage site to prevent cleavage) in the presence of 10 mM Mg(II) and 50 mM PIPES, pH 6.5.

Figure 4

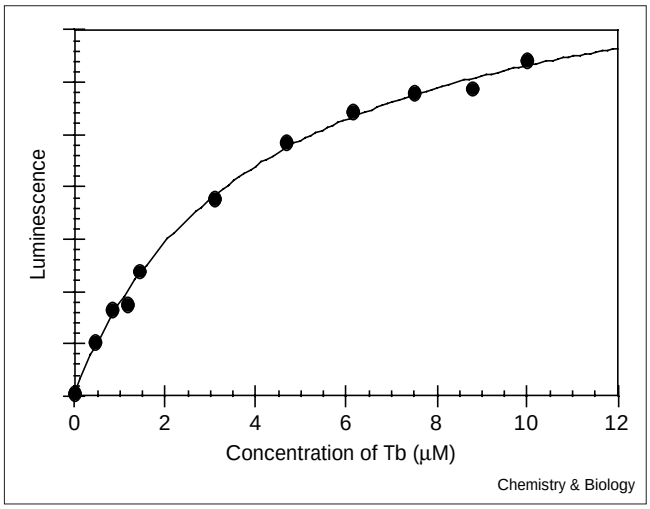

Luminescence titration of Tb(III) binding in the presence of 10 mM $MgCl_2$, 10 μM HH16 (containing a dC residue at the cleavage site) and 50 mM PIPES, pH 6.5. Data were fit to a standard binding isotherm providing a dissociation constant of 4.2 ± 0.5 μM.

has been used in qualitatively similar experiments. In the case of Eu(III), the emission bands occur at different wavelengths, but the behavior is otherwise analogous.

Förster-type energy transfer occurs with a r^{-6} distance dependence (where r is the distance between the energy donor and the energy acceptor), which means that ions free in solution should not give any signal in this experiment. Observation of Tb(III) emission indicates that the ion binds to the RNA, consistent with the fact that Tb(III) and Eu(III) are both effective inhibitors of the ribozyme cleavage reaction. More importantly, however, the steady-state luminescence can be used to monitor Tb(III) binding, allowing the determination of dissociation constants under a prescribed set of conditions. The results of such a titration experiment show that the luminescence intensity increases as a function of the Tb(III) concentration until saturation of the binding site(s) occurs (Figure 4). Nonlinear least-squares curve-fitting analysis of this experiment provides a dissociation constant of 4.2 ± 0.5 μM (10 mM Mg(II), 50 mM MES, pH 6.0, total ionic strength, I = 150 mM). This value agrees well with previously reported experiments measuring inhibition of hammerhead cleavage by Tb(III) in which a $K_{i,app}^{Tb}$ of 1.0 ± 0.2 μM was measured under similar conditions (10 mM Mg(II), 50 mM PIPES, pH 7.5, I = 150 mM) [20]. If the titration curve is extended beyond 15 μM $TbCl_3$ in the presence of 10 mM $MgCl_2$, an additional increase in luminescence intensity occurs. This feature cannot be saturated in the accessible concentration range indicating that there are other sites on the hammerhead ribozyme to which Tb(III) binds, but with a weaker affinity. Higher concentrations of Tb(III) or reduced concentrations of Mg(II) favor population of these additional sites.

Luminescence lifetime measurements

The luminescence lifetime of lanthanide ions in aqueous solution can provide information regarding the inner-sphere coordination environment of the ion [28–30]. The primary pathway for nonradiative decay of the lanthanide ion excited state is through the O–H vibrational manifold of bound water molecules. The difference in the luminescence decay rate (τ^{-1}) in H_2O versus D_2O has been shown empirically to vary linearly with the number of water molecules, q, in the inner coordination sphere:

$$q = A^{*}\left(\tau_{H_2O}^{-1} - \tau_{D_2O}^{-1}\right) \quad (1)$$

where τ_{D_2O} is the luminescence lifetime in D_2O and τ_{H_2O} is the lifetime in H_2O [30]. The constant A is 4.2 for Tb(III) and 1.05 for Eu(III) for τ^{-1} values in ms^{-1} [29]. Figure 5a shows the luminescence decay for the Tb(III) excited state while bound to the hammerhead ribozyme in water and D_2O measured by sensitized emission. As expected, the luminescence lifetime in D_2O is much longer than in water. Both curves fit well to single exponential decays giving the lifetimes listed in Table 1. As shown in Figure 5b, this experiment indicates that 6.0 ± 0.5 water molecules coordinate to the Tb(III) ion while bound to the RNA. As the aqua ion of Tb(III) is 9 coordinate, these data indicate that three water molecules are displaced when the ion binds to RNA. Comparable experiments using Eu(III) found that 4.7 ± 0.5 water molecules were bound to the ion. As Eu(III)

Figure 5

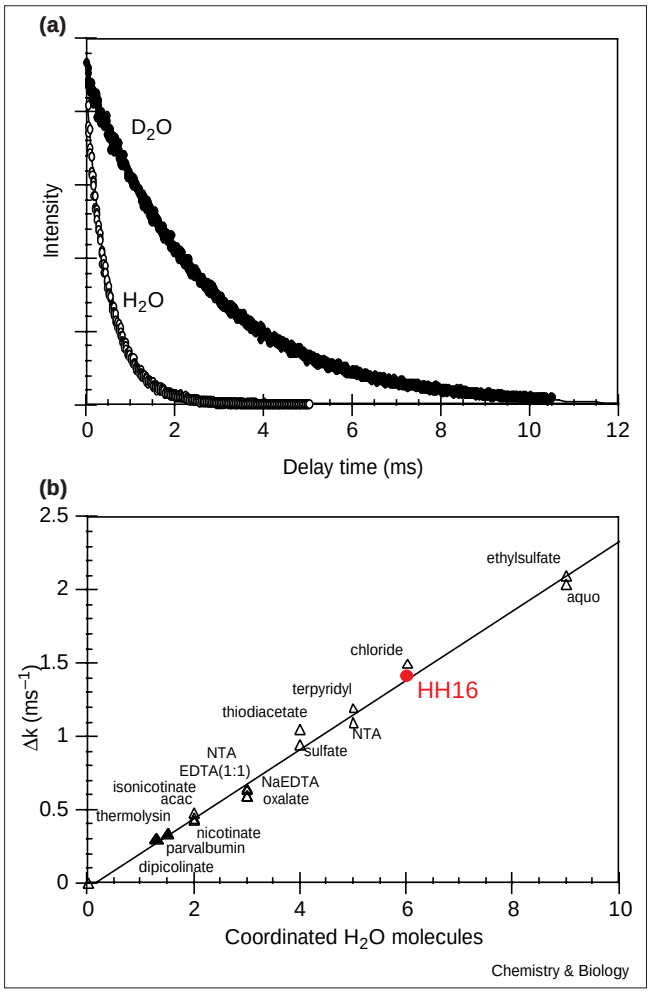

Luminescence lifetime studies for Tb(III) bound to HH16. (a) Lifetime time course for Tb(III) fit to a single exponential decay. Excitation was at 260 nm and emission was followed at 544 nm. Each point is the average of 25–100 flashes and lifetime integration was followed for a total of 10–20 ms depending on the lifetime. The sample contained 10 μM Tb(III), 10 mM Mg(II), 10 μM HH16 (containing a dC residue at the cleavage site) and 50 mM PIPES buffer, pH (or pD) 6.5. (b) Correlation of the difference in lifetime decay rates with known Tb(III) complexes (△) or Tb(III) adducts of metalloenzymes (▲). Data for the correlation were taken from [30].

aqua ions are 8–9 coordinate this again corresponds to the loss of the three or four water molecules upon binding to the RNA. It is unclear whether the lower hydration is a factor in the less efficient inhibition observed for Eu(III).

Direct excitation experiments

The $^7F_0 \rightarrow {}^5D_0$ transition for Eu(III) ions is sensitive to the coordination environment of the ion [28,29]. Because both levels are nondegenerate, the number of peaks in the excitation spectrum corresponds to the minimum number of unique environments present in solution. Figure 6 shows a wavelength scan measured over the frequency range

Table 1

Luminescence lifetimes and decay constants for the HH16 adducts of Tb(III) and Eu(III).

Ion	Solvent	τ (ms)	τ^{-1} (ms^{-1})	$\tau^{-1}_{H_2O} - \tau^{-1}_{D_2O}$	Number of coordinated waters, q
Tb(III) sensitized emission	H_2O	0.53	1.89	1.42	6.0 ± 0.5
	D_2O	2.12	0.47		
Eu(III) sensitized emission	H_2O	0.20	5.0	4.35	4.6 ± 0.5
	D_2O	1.55	0.65		
Eu(III) direct excitation	H_2O	0.206	4.85	44.4	4.7 ± 0.5
	D_2O	2.56	0.376		

typically observed for Eu(III) compounds. Within the resolution of the experiment, a single Gaussian–Laurentzian peak [31] centered at 578.9 nm is observed when up to three equivalents of Eu(III) are added to the ribozyme solution. A small amount of asymmetry in the peak shape for the Eu(III) adduct is observed. This asymmetry may reflect a small population of a second coordination environment in the presence of more than one equivalent of Eu(III). $Eu(H_2O)_9$ exhibits a peak at 578.8 nm. The relatively high energy of the Eu(III)–RNA transition measured here, compared with typical protein bound Eu(III), is consistent with the significant number of water molecules coordinated and the absence of carboxylate coordination moieties. Eu(III) bound to oligonucleotides also exhibits signals in the same region [32,33]. The analysis of the frequency of the $^7F_0 \rightarrow {}^5D_0$ transition in terms of 'nephelauxetic parameters' of the ligating moieties [34] did not include phosphate or ketone oxygen coordinating groups, so it is impossible to make such predictions for this type of RNA binding site.

Luminescence lifetime data were collected simultaneously with the excitation wavelength scans. These data show that, under stoichiometric conditions, the decay can be accurately fit to a single exponential whether measured at the peak maximum or on the wings of the signal. The lifetimes are independent of the excitation wavelength. Because the luminescence lifetime of the Eu(III) ion is dependent upon its coordination environment, as discussed above for Tb(III), the binding of multiple ions generally leads to lifetime decay curves that are biexponential or polyexponential. This experiment therefore further supports our conclusion that there appears to be a single site which is preferentially occupied. When excess Eu(III) is added to the sample, broadening of the excitation profile is observed concomitant with multicomponent lifetime decay curves (data not shown).

On the basis of the luminescence experiments alone, one could draw two potential interactions between G5 and the

Figure 6

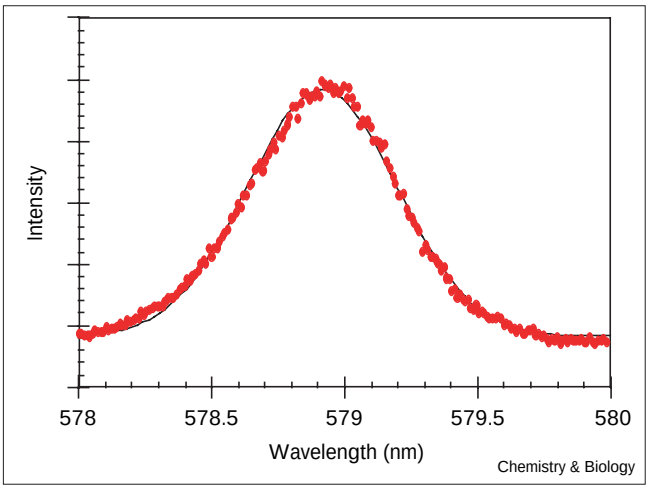

Laser excitation profile for Eu(III) bound to HH16.

Figure 7

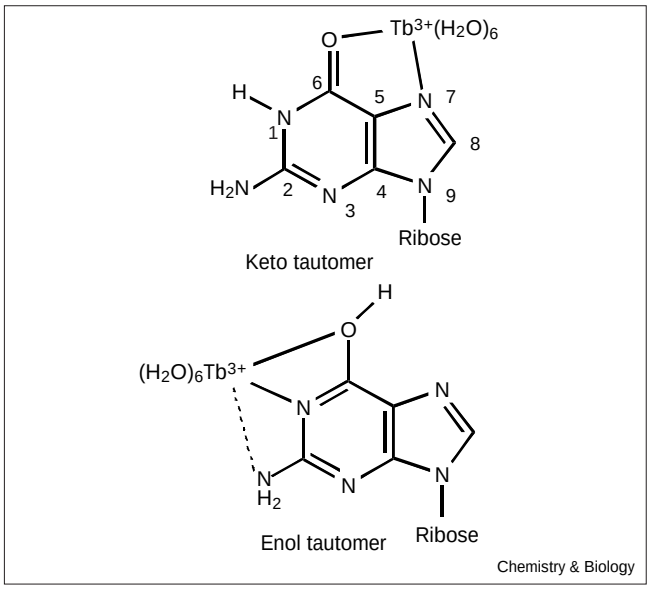

Schematic diagram of two coordination modes consistent with the Tb(III) and Eu(III) luminescence data. The enol tautomer mode is the only one that is consistent with structural data on Tb(III) binding.

inhibitory Tb(III) ion. These two options are shown in Figure 7. Both sites provide at least two inner-sphere contacts between G5 and the lanthanide ion. The identity of an additional inner-sphere ligands is not immediately obvious from the data. The chelation of metals by the N7 and O6 sites of guanosine bases is well documented [35]. In duplex regions, this binding mode is accessible to many ions without a drastic distortion of the helical structure. In the case of the hammerhead ribozyme, however, both the keto and enol sites are vacant because of the location of G5 in the uridine turn motif where the guanine base protrudes into the solvent. The N1 and O6 chelation mode is consistent with the crystallographic data on Tb(III) binding to the hammerhead, and is therefore the model we favor [20]. Furthermore, this site provides proximity to functionalities on the base of A6 as well as 2′ hydroxyl groups of positions 15.3 and 16.2. These structural features might provide additional ligands for the ion in solution in a mode that the crystal packing of the hammerhead precludes.

Metal-ion selectivity

The site-specific binding of Tb(III) adjacent to position G5 allows the use of luminescence to probe the metal ion specificity of this site. By pre-loading the site with Tb(III) followed by a titration of a competitor ion, the equilibrium between Tb(III) and any metal ion at this site can be quantified. We define the equilibrium constant that describes this competition as K_{comp}. A typical titration curve is shown in Figure 8a in which the loss of Tb(III) emission is observed upon addition of Zn(II) in the presence of constant concentrations of RNA, Tb(III), Mg(II) and Na^+. This method should be relatively insensitive to metal binding to loci other than the core Tb(III) site. Metal binding at sites other than G5 almost certainly occurs under the titration conditions. Such binding, however, will only affect the luminescence intensity when the Tb(III) ion is displaced, preventing energy transfer. Displacement can occur through a physical swap of one ion for the other, or potentially through disruption of the ribozyme structure because of denaturation or reorganization. As the luminescence intensity is insensitive to these other binding events, K_{comp} should reflect only the interaction at the Tb(III) site. The values of K_{comp} for the divalent ions tested vary over almost three orders of magnitude (Figure 8b), indicative of a highly selective site. Monovalent ions can also compete with bound Tb(III), but require very high concentrations to be effective. When the selectivity is compared with functions such as the ionic potential, a roughly linear correlation becomes evident (Figure 8c). As the ionic potential is inversely related to the pK_a of a metal aqua ion [36] as well as the free energy of hydration, ΔG_{hyd} [37], these correlations are linear as well.

In the cases of Co(II) and Zn(II), metal binding to the hammerhead ribozyme was observed crystallographically to occur at both the Watson–Crick face of G5 as well as at the N7 position [6]. Binding to the back-side of the purine ring could affect Tb(III) binding at the Watson–Crick face by inductive effects. Upon metal binding to the N7, electron density would be withdrawn from the O6 carbonyl oxygen through the purine ring system, making it a less satisfactory ligand for Tb(III). The fact that there are two modes for Co(II) and Zn(II) binding to G5 might account for their ability to compete so effectively for the Tb(III) site. Mn(II), however, has not been observed to bind to the N7 of G5 but still displays high affinity for the G5 site. $[Co(NH_3)_6]^{3+}$ also effectively competes away Tb(III),

Figure 8

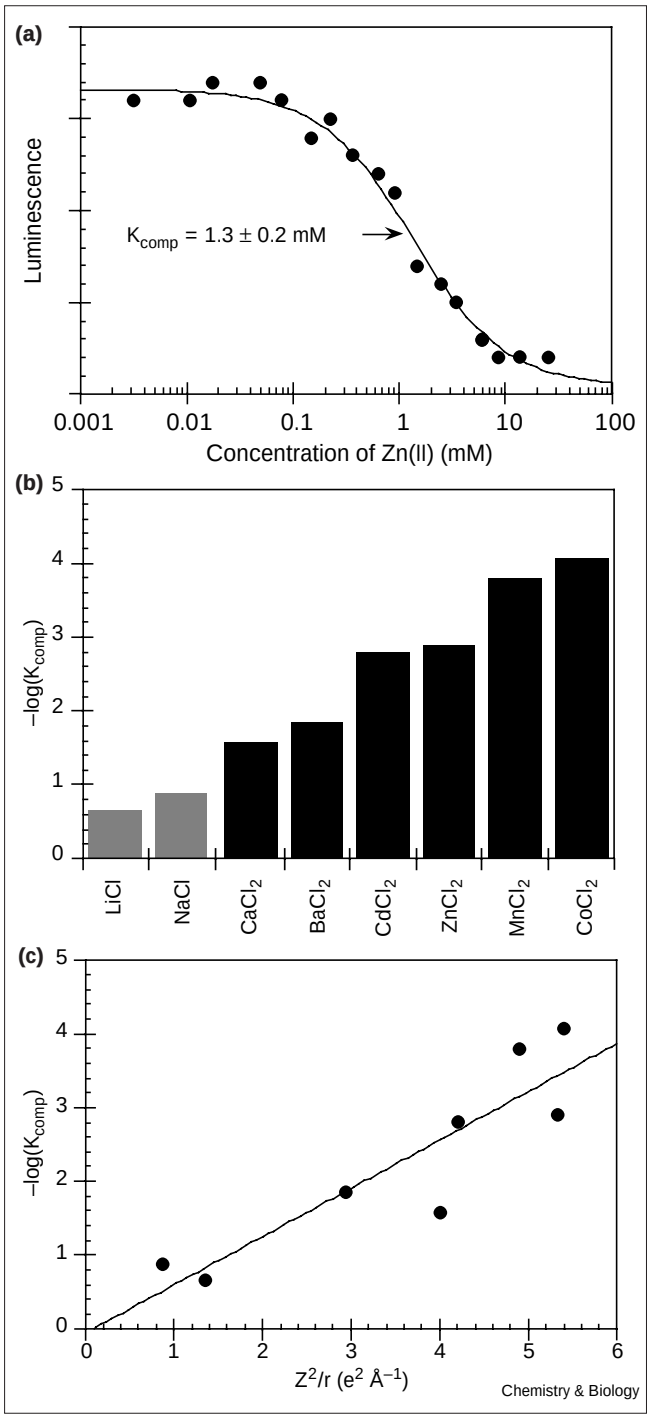

Specificity of metal binding to the site adjacent to G5. (a) A typical luminescence titration curve showing a competitor (Zn(II)) drive Tb(III) out of its binding site. Each point represents the average of four independent measurements and the curve has been fit to a standard binding isotherm as described in the Materials and methods section. (b) A histogram showing the specificity constant K_{comp} determined from titrations like that shown in (a). (c) A plot showing the correlation between the specificity constant of the binding site and an ionic potential function, Z^2/r (e^2/Å). Z is the charge of the ion and r is the radius of the ion.

indicating that inner sphere coordination is not necessarily required to displace the inhibitor.

Discussion

Luminescence spectroscopy allowed us to characterize Tb(III)- and Eu(III)-bound forms of the hammerhead ribozyme. These experiments show that a single equivalent of the lanthanide ion binds the ribozyme under conditions similar to those used for inhibition studies and that upon binding, the ion remains mostly hydrated. The luminescence data help to clarify several ambiguous issues from our crystallographic characterization of the Tb(III) binding site [20] and emphasize the need to use redundant approaches to study these metal–RNA interactions.

From the crystallographic study, it was somewhat unclear whether one or more Tb(III) ions are bound to the ribozyme. Three regions of electron density were observed when studied by co-crystallization, but only a single feature resulted from soaking crystals in concentrated $TbCl_3$ solutions [20]. The 15.3 2′-acetamide modification studies showed biochemically that the G5 site was important for inhibition, but could not address whether binding occurred at the other two sites. The luminescence titrations and the singular feature in the excitation profile both support the hypothesis that, under the inhibition conditions, only a single lanthanide ion binds to the hammerhead ribozyme. The other features in the electron-density map therefore most likely result from the extremely high concentrations of $TbCl_3$ used for the crystallographic experiments. Under these conditions, binding occurs at some of the lower affinity sites that are not involved in the inhibition of cleavage.

The lifetime experiments in water and D_2O address another ambiguity remaining from our earlier work. In the crystallographic study, the resolution was insufficient to observe the waters of hydration around the Tb(III) ion. Furthermore, the electron-density peak was located with its center 3.8 and 3.9 Å from its closest contacts with the RNA. These contacts are the N1 and N2 positions of G5, respectively. These distances are too long for inner-sphere Tb(III) binding; typical water ligands have Tb(III)–OH_2 distances of approximately 2.4 Å [38]. The luminescence experiments indicate that Tb(III) makes 2–3 inner sphere contacts with the RNA when it binds. The spectroscopic data were collected under conditions similar to those used for the inhibition studies and are probably more representative of the mechanistically relevant interactions than the crystallographic data. In this case, crystallography was an excellent method to identify the overall binding site, but the manner in which the metal ion binds to the site may be perturbed by the high ionic strength conditions required for crystal growth. This contrast between the spectroscopic and structural studies highlights an important point with respect to analyzing crystallographically determined metal-binding

sites within RNA structures. Because there is a significant ionic component to the binding of these ions to the RNA, solution conditions can have a significant impact on the metric parameters within these sites. Furthermore, extremely high concentrations of ions are used to insure that binding sites are fully populated. These conditions obviously provide no information regarding the thermodynamics of the binding event(s) nor relative affinities when there are multiple sites.

Luminescence spectroscopy has been used previously to study the binding of lanthanide ions to tRNA [39–42]. These studies were prompted by the fact that three Mg(II) ions are replaced by Sm(III) in the crystal structure of yeast $tRNA^{Phe}$ [43]. Luminescence data for Eu(III) and Tb(III) binding to $tRNA^{Phe}$ were consistent with the X-ray crystallography. Titration curves showed that three equivalents of Eu(III) are bound to the RNA [41,42], and the lifetime data indicated that the interaction was primarily outer-sphere. In one study, 5.9–6.3 water molecules were coordinated to each bound Eu(III) ion [42]. In a second study, the number of water molecules bound to the Eu(III) ion varied from 4.5 to 6.3, depending on the amount of Eu(III) present [41]. This shift in q implies the presence of multiple sites with different levels of hydration. The examination of these sites could not progress any further for two reasons. First, there was no easy way to determine biochemically the role of these particular metal-binding sites. Second, because there were three sites with comparable affinities, the specificity of any single site was difficult to address.

The Eu(III) data presented in this study are very similar to what was observed for tRNA. The single feature in the hammerhead ribozyme excitation profile corresponds exactly to one of the curve-resolved components of the slightly asymmetric $^7F_0 \rightarrow {}^5D_0$ excitation peak observed when four equivalents of Eu(III) were added to $tRNA^{Phe}$ [42]. It is possible that there are unresolved components in the hammerhead excitation spectrum, but the single exponential decay of the lifetime data indicates that these unresolved components must have very similar coordination environments. These additional binding events are evident in the presence of higher concentrations of Eu(III), as expected, because of the population of additional sites with lower affinities. These other sites may include those observed in the co-crystallization experiments [20].

The fact that the dominant Tb(III) binding site on the hammerhead ribozyme is adjacent to an unpaired guanine correlates nicely with several other studies of Tb(III) binding to nucleic acids. Yonuschot and coworkers [44] found that Tb(III) binding to polyG was much more efficient than to other homopolymer RNAs. Furthermore, sensitized emission was shown previously to occur in the presence of single-stranded DNAs, especially those that contain guanine bases [45,46], but the emission from duplex sequences is minimal [47]. These results support the idea that Tb(III) coordination to the nucleobase is required for efficient energy transfer and that coordination to the phosphate backbone alone is, therefore, insufficient for sensitization [48,49]. Recently, the efficiency of energy transfer from mononucleotides and DNA to Tb(III) has been studied as well [47]. Of the mononucleotides, dGMP has the greatest ability to sensitize Tb(III) luminescence. G·G mismatches within duplexes are also efficient sensitizers.

The differential efficiency of the bases with respect to their energy transfer to Tb(III) clearly represents a potential pitfall in the use of sensitized emission luminescence spectroscopy. In the case of an RNA with two or more Tb(III) binding sites, sensitized emission experiments might report inhomogeneously about their populations. A less populated site that has more efficient energy transfer properties might dominate a signal even in the presence of a more highly populated site if the latter is a poor sensitizer. For this reason, direct excitation experiments and additional biochemical or structural approaches should be considered essential for characterizing lanthanide binding sites to highly structured RNAs where the presence of multiple binding sites is considered likely. In the case of the hammerhead ribozyme, two of the three Tb(III) binding sites observed crystallographically involved only phosphate coordination. On the basis of the studies described above, the sensitization efficiency will be significantly lower for these sites and binding might potentially have been missed had only sensitized emission been employed. The direct excitation experiments, however, do not require this energy transfer pathway. The finding that the direct excitation and the sensitized emission experiments for Eu(III) provide comparable results suggests that the same metal-binding site is observed in both cases.

For the G5 site, the relative affinity correlates with the Z^2/r value of the ion, a charge radial function sometimes called the ionic potential. One other study has looked at the specificity of an RNA metal-binding site, one found on the P4–P6 domain of the group I intron from *Tetrahymena* [37,50]. This study probed K^+ binding adjacent to the three A-platforms by nucleotide analog interference mapping. Preferential binding of K^+ occurs here, even in the presence of Mg(II), Mn(II) or other monovalent ions. These A-platform related sites are highly organized; each example making five inner-sphere contacts with RNA derived ligands, only one of which is a phosphate oxygen. The relative affinities for several ions binding to one of the three A-platform sites were determined and they exhibited a similar correlation to the one shown here for the hammerhead ribozyme G5 site. The physical basis of this correlation may relate to hydration of the ion because the binding event is actually a competition between water and RNA ligands. The selectivity between K^+ and Na^+ in

G-quartet structures has been shown to relate to the relative free energies of hydration [51]. The energetic cost of dehydration based on classical theory is given by:

$$-\Delta G_{hyd} = 164(Z^2)/r \quad (2)$$

where Z is the charge of the ion, r is the radius of the ion in Å and ΔG is in kcal/mol at 25°C [37]. The quandary, however, is why do sites that remain predominantly hydrated, such as the G5 site from the hammerhead ribozyme, have affinities related to the hydration energy? To our knowledge, the specificity of only the two metal-binding sites discussed above have been measured. With such a small basis set, it is impossible to generalize a trend. Several more metal-binding sites must be identified on RNAs and studied in this manner. One can speculate, however, that this correlation might hold for one class of sites. The structural features that might define such a class, however, are entirely unknown.

As the G5 metal-binding site is one of the best characterized in the field of RNA–metal interactions, it is worthwhile comparing this site with those from typical metalloproteins. One of the primary differences is the extent of hydration. In a recent survey of the protein crystal structures containing Mg(II), the majority of the sites had two or fewer water ligands [52]. The rest of the coordination sites were occupied by proteinaceous donors. Most commonly, these ligands are carboxylates for Mg(II), but a variety of other donors are observed. In the case of RNAs, such a systematic search is more complicated because of the low resolution common to most of these structures and the fact that Mg(II) ions are often defined on the basis of their hydration patterns in the first place. The majority of the Mg(II) sites, however, have four or more water ligands and therefore make many fewer direct interactions with the RNA. The G5 site of the hammerhead ribozyme is no exception. In the crystallographic experiments, the waters of hydration were not defined for any of the metal ions that bind to this site. However, the location of the site on the solvent-exposed surface of the molecule without clear contacts to donors from the RNA implies significant hydration. The lanthanide ions make 2–3 inner sphere contacts with the RNA. It is unlikely that a smaller Mg(II) ion would have more inner sphere interactions in this site than either Tb(III) or Eu(III) and it is possible that it would have even fewer contacts.

It is not immediately obvious why the metal-binding sites on RNAs tend to be more hydrated than equivalent protein examples. It might relate to the larger size of the monomeric units in nucleic acids and the fewer degrees of geometric freedom available to accommodate an octahedrally coordinated Mg(II) ion. Furthermore, the large negative charge of the nucleic acid molecules as a whole leads to extensive nonspecific binding of ions, a problem rarely encountered in the study of metalloproteins. The consequences of the less well-defined sites are quite striking. In general, these ions are much less tightly coordinated to the RNA than they would be to a protein-binding site. Furthermore, the ability to make substitutions into these binding sites is quite extensive. Of the many metal-binding sites on a typical RNA, it is likely that inhibition results from improper binding in just one or two of the individual sites in any given case. In the rest of the sites the substitution may be quite benign.

Significance

Metal ions have a role in the catalysis and in maintaining the structure of the hammerhead ribozymes but little is known about the nature of the binding of metals to the ribozyme. The tools of luminescence spectroscopy can be used to probe a metal-binding site on the hammerhead ribozyme. The crystallographic studies that originally located the Tb(III)-binding site were not of sufficiently high resolution to allow the determination of the inner-sphere ligands of the ion. Furthermore, as the crystals were grown in 1.8 M Li_2SO_4, the details of the coordination environment may not be identical to those observed under conditions where Tb(III) inhibition occurs. Our studies support the notion that Tb(III) inhibition occurs through site-specific binding of the ion. Binding appears to occur through 2–3 inner-sphere interactions in the case of Tb(III) as opposed to the outer-sphere binding mode observed in the crystallographic studies. The ability to use Tb(III) as a probe for the binding of other ions to this site allows us to compare the metal-binding affinities of a number of ions to the RNA. The hammerhead ribozyme shows a remarkable degree of selectivity at this site in spite of the fact that many ions are capable of activating the cleavage chemistry. The selectivity appears to correlate best with the ionic potential. As other metal-binding sites are identified for spectroscopic analysis, it will be important to see if the correlation is general or whether each metal-binding site behaves differently in terms of their patterns of molecular ionic recognition.

Materials and methods

Reagents

Water was purified by using a Milli-Q (Millipore) filtration system and then autoclave sterilized prior to use. D_2O (99.9%, Cambridge Isotope Labs) was filter sterilized through 0.2 μm syringe tip units (Advantec MFS, Inc). For the extremely sensitive laser excitation experiments, these filter tips had to be prewashed with 2–3 ml of solution to avoid trace contamination with EDTA. All chemicals were purchased as the highest purity available from commercial sources and solutions were sterile filtered prior to use. Titration against EDTA with Arsenazo I as the indicator allowed the determination of the exact concentration of lanthanide ion stock solutions after sterile filtration [53]. T7 RNA polymerase was purified by standard procedures from an *Escherichia coli* strain transfected with a plasmid containing the RNAP and ampicillin resistance genes [54].

Preparation of RNA

Spectroscopic studies were conducted with the hammerhead 16 (HH16) construct which has been previously described and characterized [3].

The ribozyme strand was synthesized by *in vitro* T7 RNA polymerase transcription off of a synthetic DNA template [55]. Top strand DNA (600 nM) was annealed to the template (300 nM) by heating to 90°C for 90 s in a buffer containing 40 mM Tris Buffer, pH 8.1, 20 mM $MgCl_2$, 0.1% Triton X-100, 1 mM spermidine, 5 mM DTT and then cooled to 37°C. Nucleotide triphosphates (Sigma) were added as 100 mM stock solutions (neutralized to pH ~7.0) to a final concentration of 2 mM for CTP, UTP and ATP and 3 mM for GTP. T7 RNA polymerase was added to a final concentration of 30 μg/ml. Transcriptions were incubated at 37°C for 3–4 h. The reactions were centrifuged to separate the insoluble magnesium pyrophosphate from the soluble RNA. Transcription products were purified by ethanol precipitation of the RNA followed by polyacrylamide gel electrophoresis on 15% gels. The full length RNA was eluted from the gel into 0.5 M sodium acetate overnight at 4°C and separated from the gel matrix by filtration. The RNA product was isolated by ethanol precipitation from this solution and stored frozen in sterile deionized water. RNA concentrations were determined based upon OD_{260} using an approximation for the extinction coefficient of 10,000 M^{-1} cm^{-1} per nucleotide. In certain cases, a minor EDTA contamination was observed in laser excited luminescence experiments. For these samples, RNA was passed through a G25 micro-spin column (Pharmacia Biotech) pre-equilibrated 5 times with sterile deionized water. These samples were then concentrated in a Speed-Vac concentrator (Savant) to their final concentration.

The substrate strand was chemically synthesized by standard methodologies with either N-acetyl or N-benzoyl phosphoramidites (Glen Research) on an Applied Biosystems ABI-394 automated RNA synthesizer. In many cases, a noncleavable substrate analog was requires to prevent ribozyme activity and allow spectroscopic measurement. A single deoxy-cytosine was therefore incorporated at the cleavage site in these cases. Synthetic oligonucleotides were deprotected in one of two fashions, depending on the protecting groups. N-acetyl oligos were treated with 1 ml 40% methylamine in water (Fluka) for 15 min at 65°C. The methylamine solution containing the RNA was separated from the CPG support and concentrated until dry in a Speed-vac concentrator. Treatment of the partially deprotected RNA with 20 equivalents 1.4 M HF in N-methyl pyrrolidone for 1.5 h at 65°C completed the deprotection process. This solution was diluted to 1 ml and desalted by passing the RNA through a NAP-10 (Pharmacia) column. The RNA was further purified by ethanol precipitation and then gel electrophoresis on 20% gels as described above for the transcribed RNA. N-benzoyl oligos were treated with 4 ml 3.7 M NH_4OH in MeOH (1:3 v/v dilution of concentrated NH_4OH) for 18 h at 55°C. The methanolic ammonia containing the RNA was separated from the CPG support and the solvent was then removed in a Speed-Vac concentrator. The RNA was solubilized in 1 ml 1 M tetraethylammonium fluoride (Aldrich) and incubated at 37°C for 18 h. The deprotected RNA was then desalted and purified as described above.

Luminescence lifetime measurements

Luminescence lifetime measurements for Tb(III) bound to RNA were conducted with a Spex 1681 0.22 m Fluorolog fluorometer fitted with a Spex 19340 phosphorimeter flash lamp. Typical samples contained 1 μM HH16 Ribozyme and 1 μM HH16 dC9 non-cleavable substrate analog in a 50 mM PIPES buffer, pH (or pD) 6.5 containing 10 mM $MgCl_2$ and 10 μM $TbCl_3$. 260 nm excitation was used with an average flash pulse length of 3 μs. 544 nM emission was monitored as a function of the delay time between the excitation and the emission. Emission intensity data were collected and integrated out to 20 ms under all conditions and averaged over 25–100 flashes. The lifetime curves were fitted to standard first-order exponential decay equations using the program Kaleidagraph (Synergy Software) to obtain a rate constant for the luminescence decay.

Laser-excited luminescence

Data were collected essentially as previously described [56]. Briefly, 10 μM samples of HH16 in 50 mM PIPES, pH 6.5, 10 mM $MgCl_2$ and variable amounts of $EuCl_3$ were illuminated with 578–581 nM light from a Continuum YG-581 pulsed (10 Hz) Nd:YAG laser pumped tunable TDL-50 dye laser, while monitoring the emission at 614 nm. Single photon counting data were collected by a LeCroy data acquisition system interfaced to a Swan 386SX computer. Raw intensity data were corrected for fluctuations in the laser power. Excitation data were then fit to Gaussian-Laurentzian functions which describe the line shape of Eu(III) excitation spectra [31]. Non-linear least-squares regressions were performed by using the program Kaleidagraph. Lifetime data were fit in a similar manner to standard exponential decay equations.

Measurement of the Tb(III) affinity constant by luminescence titration

Affinity measurements for Tb(III) binding to HH16 were measured by titration of $TbCl_3$ into RNA solutions while monitoring the sensitized emission of Tb(III) at 544 nm. Samples of HH16 (1 μM in 50 mM PIPES, pH 6.5 and 10 mM $MgCl_2$) containing a dC residue at the cleavage site were used to prevent ribozyme cleavage. $TbCl_3$ was titered in as a 100 μM solution containing ribozyme buffer and $MgCl_2$ such that despite the volume changes, only the Tb(III) concentration varied. Data are presented as the average of four measurements.

Metal competition studies

Metal competition studies were conducted in a manner similar to the Tb(III) titrations. The initial samples contained pre-annealed HH16 ribozyme (1 μM) with the dC9 noncleavable substrate analog (1 μM) in 50 mM MES, pH 6.0, I = 150 mM, 10 mM $MgCl_2$ and 10 μM $TbCl_3$. The slightly lower pH was used to avoid complications associated with metal hydroxide precipitation for some of the competitors used. Titrants containing 1 μM–1 M competitor in a 1 × ribozyme sample were titrated into the sample cuvette. This procedure allowed for the addition of significant volumes of titrant without changing the concentrations of ribozyme, Tb(III) or Mg(II) in the sample. Samples were irradiated at 290 nm and 544 nm emission was monitored. Relative luminescence data were averaged over four trials and fit to equation 3 by using the program Kaleidagraph:

$$L_i = L_\infty + \Delta L \bullet \left(1 - \frac{[\text{Metal}]_i}{[\text{Metal}]_i + K_{comp}}\right) \quad (3)$$

where L_i is the luminescence intensity at some concentration i of total added competitor ion, L_∞ is the background luminescence in the presence of a saturating concentration of the competitor, ΔL is the total change in luminescence intensity over the titration and K_{comp} is the affinity constant for the exchange of the two metal ions. The value K_{comp} correlates with the dissociation constants for the competitor ion (M^{y+}_{comp}) and Tb(III) based upon equation 4:

$$K^{Metal}_{comp} = \frac{K_d^{Tb(III)}}{K_d^{Metal}} = \frac{[RNA \bullet M^{y+}_{comp}]([Tb(III)]_{total} - [RNA \bullet Tb(III)])}{[RNA \bullet Tb(III)]([M^{y+}_{comp}]_{total} - [RNA \bullet M^{y+}_{comp}])} \quad (4)$$

Acknowledgements

This work was supported by the NSF (CHE-9504698 to A.L.F. and CHE-9705788 to W.D.H.), the NIH (GM-36944 to O.C.U.) and the Colorado RNA Center. We would also like to thank Evelyn Jabri for her helpful discussions.

References

1. McKay, D.B. & Wedekind, J.E. (1998). Small ribozymes. In *The RNA World.* (Gesteland, R., Cech, T., & Atkins, J., eds) pp. 265-286, Cold Spring Harbor Laboratory, Cold Spring Harbor, NY.
2. McKay, D.B. (1996). Structure and function of the hammerhead ribozyme: an unfinished story. *RNA* 2, 395-403.
3. Hertel, K.J., Herschlag, D. & Uhlenbeck, O.C. (1994). A kinetic and thermodynamic framework for the hammerhead ribozyme reaction. *Biochemistry* 33, 3374-3385.
4. Heidenreich, O. & Eckstein, F. (1997). Synthetic ribozymes: the hammerhead ribozyme. In *Concepts in Gene Therapy.* (Strauss, M. & Barranger, J., eds.) pp. 169-195, Walie de Gruyter, Berlin.
5. Thomson, J.B., Tuschl, T. & Eckstein, F. (1996). The hammerhead ribozyme. In *Catalytic RNA.* (Lilley, D.M.J. & Eckstein, F., eds) pp. 173-196, Springer-Verlag, Berlin.

6. Murray, J.B., *et al.,* & Scott, W.G. (1998). The structural basis of hammerhead ribozyme self-cleavage. *Cell* **92**, 665-673.
7. Scott, W.G., Finch, J.T. & Klug, A. (1995). The crystal structure of an all-RNA hammerhead ribozyme: a proposed mechanism for RNA catalytic cleavage. *Cell* **81**, 991-1002.
8. Scott, W.G., Murray, J.B., Arnold, J.R.P., Stoddard, B.L. & Klug, A. (1996). Capturing the structure of a catalytic RNA intermediate: the hammerhead ribozyme. *Science* **274**, 2065-2069.
9. Pley, H.W., Flaherty, K.M. & McKay, D.B. (1994). Three-dimensional structure of a hammerhead ribozyme. *Nature* **372**, 68-74.
10. Dahm, S.C. & Uhlenbeck, O.C. (1991). Role of divalent metal ions in the hammerhead RNA cleavage reaction. *Biochemistry* **30**, 9464-9469.
11. Feig, A.L. & Uhlenbeck, O.C. (1998). The role of metal ions in RNA biochemistry. In *The RNA World.* (Gesteland, R., Cech, T., & Atkins, J., eds) pp. 287-319, Cold Spring Harbor Laboratory, Cold Spring Harbor, NY.
12. Long, D.M., LaRiviere, F.J. & Uhlenbeck, O.C. (1995). Divalent metal ions and the internal equilibrium of the hammerhead ribozyme. *Biochemistry* **34**, 14435-14440.
13. Pan, T., Long, D.M. & Uhlenbeck, O.C. (1993). Divalent metal ions in RNA folding and catalysis. In *The RNA World.* (Gesteland, R. & Atkins, J., eds) pp. 271-302, Cold Spring Harbor Laboratory, Cold Spring Harbor, NY.
14. Pyle, A.M. (1993). Ribozymes: a distinct class of metalloenzymes. *Science* **261**, 709-714.
15. Pyle, A.M. (1996). Role of metal ions in ribozymes. In *Interactions of metal ions with nucleotides, nucleic acids, and their constituents, Metal Ions in Biological Systems Vol. 32.* (Sigel, A. & Sigel, H., eds.) pp. 479-520, Marcel Dekker, New York.
16. Peracchi, A., Beigelman, L., Scott, E.C., Uhlenbeck, O.C. & Herschlag, D. (1997). Involvement of a specific metal ion in the transition of the hammerhead ribozyme to its catalytic conformation. *J. Biol. Chem.* **272**, 26822-26826.
17. Ruffner, D.E. & Uhlenbeck, O.C. (1990). Thiophosphate interference experiments locate phosphates important for the hammerhead RNA self-cleavage reaction. *Nucleic Acids Res.* **18**, 6025-6029.
18. Knöll, R., Bald, R. & Fürste, J.P. (1997). Complete identification of non-bridging phosphate oxygens involved in hammerhead cleavage. *RNA* **3**, 132-140.
19. Scott, E.C. & Uhlenbeck, O.C. (1999). A re-investigation of the thio effect at the hammerhead cleavage site. *Nucleic Acids Res.* **27**, 479-484.
20. Feig, A.L. Scott, W.G., & Uhlenbeck, O.C. (1998). Inhibition of the hammerhead ribozyme cleavage reaction by site-specific binding of Tb(III). *Science* **279**, 81-84.
21. Ruffner, D.E., Stormo, G.D. & Uhlenbeck, O.C. (1990). Sequence requirements of the hammerhead RNA self-cleavage reaction. *Biochemistry* **29**, 10695-10702.
22. Tuschl, T., Ng., M.M.P., Pieken, W., Benseler, F. & Eckstein, F. (1993). Importance of exocyclic base functional groups of central core guanosines for hammerhead ribozyme activity. *Biochemistry* **32**, 11658-11668.
23. Fu, D.-J., Rajur, S.B. & McLaughlin, L.W. (1993). Importance of specific guanosine N7-nitrogens and purine amino groups for efficient cleavage by a hammerhead ribozyme. *Biochemistry* **32**, 10629-10637.
24. Slim, G. & Gait, M.J. (1992). The role of the exocyclic amino groups of conserved purines in hammerhead ribozyme cleavage. *Biochem. Biophys. Res. Commun.* **183**, 605-609.
25. Bassi, G.S., Møllegaard, N.-E., Murchie, A.I.H., von Kitzing, E. & Lilley, D.M.J. (1995). Ionic interactions and the global conformations of the hammerhead ribozyme. *Nat. Struct. Biol.* **2**, 45-55.
26. Bassi, G.S., Murchie, A.I.H. & Lilley, D.M.J. (1996). The ion-induced folding of the hammerhead ribozyme: core sequence changes that perturb folding into the active conformation. *RNA* **2**, 756-768.
27. Bassi, G.S., Murchie, A.I.H., Walter, F., Clegg, R.M. & Lilley, D.M.J. (1997). Ion-induced folding of the hammerhead ribozyme: A fluorescence resonance energy transfer study. *EMBO J.* **16**, 7481-7489.
28. Horrocks, W.D., Jr. (1993). Luminescence spectroscopy. *Methods Enzymol.* **226**, 495-538.
29. Horrocks, W.D., Jr. & Albin, M. (1991). Lanthanide ion luminescence in coordination chemistry and biochemistry. *Prog. Inorg. Chem.* **31**, 1-104.
30. Horrocks, W.D., Jr. & Sudnick, D.R. (1979). Lanthanide ion probes of structure in biology. laser-induced luminescence decay constants provide a direct measure of the number of metal-coordinated water molecules. *J. Am. Chem. Soc.* **101**, 334-340.
31. McNemar, C.W. & Horrocks, W.D., Jr. (1989). The resolution of laser-induced Eu(III) ion excitation spectra through the use of the Marquardt nonlinear regression method. *Appl. Spectrosc.* **43**, 816-821.
32. Klakamp, S.L. & Horrocks, W.D., Jr. (1992). Lanthanide ion luminescence as a probe of DNA structure. 1. Guanine-containing oligomers and nucleotides. *J. Inorg. Biochem.* **46**, 175-192.
33. Klakamp, S.L. & Horrocks, W.D., Jr. (1992). Lanthanide ion luminescence as a probe of DNA structure. 2. Non-guanine-containing oligomers and nucleotides. *J. Inorg. Biochem.* **46**, 193-205.
34. Frey, S.T. & Horrocks, W.D., Jr. (1995). On correlating the frequency of the $^7F_0 \rightarrow {}^5D_0$ transition in Eu(III) complexes with the sum of nephelauxetic parameters for all of the coordinating atoms. *Inorg. Chim. Acta* **229**, 383-390.
35. Kazakov, S.A. (1996). Nucleic acid binding and catalysis by metal ions. In *Bioorganic Chemistry: Nucleic Acids.* (Hecht, S.M., ed.) pp. 244-477, Oxford University Press, New York.
36. Huheey, J.E. (1983). *Inorganic Chemistry.* (Third Edition edn.), Harper & Row, New York.
37. Draper, D.E. & Misra, V.K. (1998). RNA shows its metal. *Nat. Struct. Biol.* **5**, 927-930.
38. Ma, J.-F., Jin, Z.-S. & Ni, J.-Z. (1994). Terbium p-nitrobenzoate hydrate. *Acta Crystallogr. C* **50**, 1008-1010.
39. Kayne, M.S. & Cohn, M. (1974). Enhancement of Tb(III) and Eu(III) fluorescence in complexes with *E. coli* tRNA. *Biochemistry* **13**, 4159-4165.
40. Wolfson, J.M. & Kearns, D.R. (1974). Europium as a fluorescent probe of metal binding sites on tRNA. I. Binding to *E. coli* formylmethionine tRNA. *J. Am. Chem. Soc.* **96**, 3653-3654.
41. Draper, D.E. (1985). On the coordination properties of Eu(III) bound to tRNA. *Biophys. Chem.* **21**, 91-101.
42. Cornwall, E.H. (1993) *Lanthanide Ions as Luminescent Probes of the Magnesium Ion Binding Sites in Yeast tRNA^{Phe}.* Ph.D. Thesis, Pennsylvania State University.
43. Jack, A., Ladner, J.E., Rhodes, D., Brown, R.S. & Klug, A. (1977). A crystallographic study of metal-binding to yeast phenylalanine tRNA. *J. Mol. Biol.* **111**, 315-328.
44. Yonuschot, G., Helman, D., Mushrush, G., Woude, G.V. & Robey, G. (1978). Terbium as a solid state probe for RNA. *Bioinorg. Chem.* **8**, 405-418.
45. Ringer, D.P., Burchett, S. & Kizer, D.E. (1978). Use of Tb(III) fluorescence enhancement to selectively monitor DNA and RNA guanine residues and their alteration by chemical modification. *Biochemistry* **17**, 4818-4825.
46. Ringer, D.P., Howell, B.A. & Kizer, D.E. (1980). Use of terbium fluorescence enhancement as a new probe for assessing the single strand content of DNA. *Anal. Biochem.* **103**, 337-342.
47. Fu, P.K.-L. & Turro, C. (1999). Energy transfer from nucleic acids to Tb(III): Selective emission enhancement by single DNA mismatches. *J. Am. Chem. Soc.* **121**, 1-7.
48. Canfi, A., Bailey, M.P. & Rocks, B.F. (1989). Fluorescent terbium chelates derived from diethylenetriaminepentaacetic acid and heterocyclic compounds. *Analyst* **114**, 1405-1406.
49. Abusaleh, A. & Meares, C.F. (1984). Excitation and de-excitation processes in lanthaide chelates bearng aromatic sidechains. *Photochem. Photobiol.* **39**, 763-769.
50. Basu, S., *et al.,* & Doudna, J.A. (1998). A specific monovalent metal ion integral to the AA platform of the RNA tetraloop receptor. *Nat. Struct. Biol.* **5**, 986-992.
51. Hud, N.V., Smith, F.W., Anet, F.A.L. & Feigon, J. (1996). The selectivity for K^+ versus Na^+ in DNA quadruplexes is dominated by relative free energies of hydration: A thermodynamic analysis by ^{1}H NMR. *Biochemistry* **35**, 15383-15390.
52. Katz, A.K., Glusker, J.P., Beebe, S.A. & Bock, C.W. (1996). Calcium ion coordination: a comparison with that of beryllium, magnesium, and zinc. *J. Am. Chem. Soc.* **118**, 5752-5763.
53. Fritz, J.S., Oliver, R.T. & Pietrzyk, D.J. (1958). Chelometric titrations using an azoarsonic acid indicator. *Anal. Chem.* **30**, 1111-1114.
54. Davanloo, P., Rosenberg, A.H., Dunn, J.J. & Studier, F.W. (1984). Cloning and expression of the gene for bacteriophage T7 RNA polymerase. *Proc. Natl Acad. Sci. USA* **81**, 2035-2039.
55. Milligan, J.F., Groebe, D.R., Witherell, G.W. & Uhlenbeck, O.C. (1987). Oligoribonucleotide synthesis using T7 RNA polymerase and synthetic DNA templates. *Nucleic Acids Res.* **15**, 8783-8798.
56. Frey, S.T., *et al.,* & Horrocks, W.D. (1994). Characterization of lanthanide complexes with a series of amide-based macrocycles, potential MRI contrast agents, using Eu(III) luminescence spectroscopy and molecular mechanics. *Inorg. Chem.* **33**, 2882-2889.